Structural Biology

DOI: 10.1002/anie.201103980

Prediction of a Ligand-Binding Niche within a Human Olfactory Receptor by Combining Site-Directed Mutagenesis with Dynamic Homology Modeling**

*Lian Gelis, Steffen Wolf, Hanns Hatt, Eva M. Neuhaus, and Klaus Gerwert**

The mammalian olfactory system comprises a large family of G protein-coupled receptors (GPCRs) to detect and discriminate numerous volatile ligands. More than 350 human genes encode functional olfactory receptors (ORs)[1] that belong to the class A (rhodopsin-like) GPCR family.[2] Owing to difficulties with functional OR expression in heterologous systems,[3,4] only a few human ORs have been characterized to date. Most deorphanized ORs, that is, ORs with a known ligand spectrum, detect multiple chemically similar odorants,[5] and hypervariable residues in the seven transmembrane (7TM) helices (I–VII) have been postulated to form the basis for ligand specificity.[6] A prerequisite for understanding olfactory receptor selectivity is information on the spatial properties of the ligand-binding niche. Different classes of approaches have been employed for such an assessment:[7] Ligand-based approaches, such as pharmacophore modeling or quantitative structure-activity relationship (QSAR), can give valuable models of the ligand structure, which is required for discriminating activating and inactive ligands, and information on the form of the binding pocket.[8–11] Receptor-based approaches such as homology modeling create a model of the protein and the binding site explicitly,[12–18] and from this give information on ligand binding. Both techniques can be combined together.[19–22] For such receptor-based and mixed approaches, the X-ray structures of seven GPCRs have been solved to date,[23–32] but none for ORs. Previous studies have used static structural models of different ORs based on a rhodopsin[12–21] and a β_2-adrenergic receptor (B2AR)[33] template. However, most odorants are highly flexible, so assessment of the ligand/protein dynamics might be of crucial importance in understanding ligand recognition by ORs. To better understand receptor activation, we thus searched for a dynamic ligand–protein interaction pattern instead of analyzing ligand-binding in static models. Therefore, in difference to other flexible GPCR ligand pocket analysis approaches,[34–37] we use the predictive power of protein/ligand complex molecular dynamics (MD) simulations[38–40] to gain insight into the protein–odorant dynamics necessary for receptor activation.

We developed a dynamic model of the functionally well-characterized human olfactory receptor hOR2AG1.[41] We used an X-ray structure of bovine rhodopsin with 2.2 Å resolution[24] as starting structure for dynamic homology modeling of hOR2AG1, since both receptors belong to the class A GPCRs, and both harbor hydrophobic ligands. The performance of this approach was previously tested by homology modeling of the B2AR ligand-binding niche based on the rhodopsin template (see Supporting Information, Section 1 a).[40] Although the overall sequence identity among class A GPCRs is relatively low, this can be compensated for by careful incorporation of experimental information as constraints.[34] In the present study, site-directed mutagenesis and functional analysis of receptor mutants by Ca^{2+} imaging were performed for validation of the hOR2AG1 homology model. Combining both techniques in a cycle of dynamic computational predictions and experimental analysis based on site-directed mutagenesis, we were able to characterize and refine the three-dimensional structure of the

[*] Prof. Dr. K. Gerwert[+]
Lehrstuhl für Biophysik, Ruhr-University Bochum
Universitätsstrasse 150, 44780 Bochum (Germany)
E-mail: gerwert@bph.ruhr-uni-bochum.de
Homepage: http://www.bph.ruhr-uni-bochum.de/
Dr. S. Wolf,[+] Prof. Dr. K. Gerwert[+]
Department of Biophysics, CAS-Max-Planck Partner Institute for Computational Biology, Shanghai Institutes for Biological Sciences
320 Yue Yang Road, 200031 Shanghai (P.R. China)
Dr. L. Gelis,[+] Prof. Dr. H. Hatt
Lehrstuhl für Zellphysiologie
Ruhr-University Bochum (Germany)
Prof. Dr. E. M. Neuhaus[+]
Neuroscience Research Center, Cluster of Excellence NeuroCure
Charité-Universitätsmedizin Berlin
Charitéplatz 1, 10117 Berlin (Germany)
[†] L.G. and S.W. contributed equally to the technical research, E.M.N. and K.G. contributed equally to the supervision of the study.

[**] We thank H. Bartel and J. Gerkrath for their technical assistance, W. Zhang (Pharmaceutical Product Development, Inc., Beijing) for her contributions to the preliminary experiments in this study, and J. Panten (Symrise, Holzminden) and T. Gerke (Henkel, Düsseldorf) for providing odorants. Calculations were performed on the PICB HPC cluster. We are grateful to the NIC Jülich (project no. hbo26) and the RRZ Köln for providing additional computing time and U. Höweler for helpful discussion. All molecular representations were made using PyMol (DeLano Scientific). This study was supported by grants from the Deutsche Forschungsgemeinschaft to E.M.N, H.H., and K.G. (SFB642), the Ruhr-University Research School, and the Ruth und Gerd Massenberg Stiftung. S.W. is funded by a CAS Young International Scientist Fellowship. E.M.N. is funded by Exc 257 NeuroCure. K.G. acknowledges a fellowship of the Mercator foundation. L.G. performed the experimental research, S.W. performed the theoretical investigations. H.H., E.M.N., and K.G. designed and conducted the research. All authors contributed to writing the manuscript.

Supporting information (full experimental details) for this article is available on the WWW under http://dx.doi.org/10.1002/anie.201103980.

ligand-binding niche within a hOR2AG1 structural model to a new extent.

We first searched for a suitable ligand-binding cavity in our model, which was verified by experimental analysis. Simulations of the initial rhodopsin-based hOR2AG1 model (for details in modeling and template choice see Supporting Information, Section 1a) revealed a cavity between helices III, V, VI, and VII as most promising ligand binding position (cavity A in Supporting Information, Figure S1, and Section 2b). Experimental validation of the ligand binding cavity was carried out by expression of wild type (WT) and mutant *hOR2AG1* in Hana3a cells and functional characterization of recombinant receptors by single cell Ca^{2+} imaging[42,43] (see Supporting Information, Figure S2, and Section 2a).

Simulations of the ligand amylbutyrate in the putative binding cavity revealed two possible orientations, one with the ligand positioned horizontally and one vertically to the membrane plane. For verification of the binding cavity and assessment of the correct ligand orientation, we used mutations of the residues Ala104$^{3.32}$ and Val260$^{6.48}$, Ser263$^{6.51}$, Ser264$^{6.52}$, and Thr279$^{7.42}$ (Figure 1a; numbers in superscripts refers to Ballesteros–Weinstein numbering[44]), which all form contacts with the ligand in the vertical binding mode during MD simulation (more details in Supporting Information, Sections 2b and 2c). The experimental analysis of point mutated receptors hOR2AG1-A104I, -V260W, -S263V, -S264V, -S264C, and -T279V by Ca^{2+} imaging showed a decreased activity compared to the WT receptor (Figure 1b and Table 1). Therefore, the comparison of theoretical and experimental analysis revealed the proposed cavity as amylbutyrate binding niche and amylbutyrate to be bound in a vertical binding mode (Figure 1c).

A list of all putative ligand contact residues is provided in the Supporting Information, Section 3a. Ala104$^{3.32}$, Phe206$^{5.47}$, Val260$^{6.48}$, Ser263$^{6.51}$, Ser264$^{6.52}$, and Thr279$^{7.42}$ are located on sequence positions that are highly variable throughout the olfactory protein family and might therefore determine ligand specificity[6,45,46] (Supporting Information, Figure S3a, and Section 3b).

In addition, we experimentally analyzed four control mutations, A104G, F206V, V239W, and S242C, which should not have any influence on ligand binding as judged by MD simulations. In agreement with the model, in the experiment none of the control mutations affected receptor activation compared to the WT receptor (Figure 1b).

We investigated computationally if we could determine a quantitative criterion for receptor activation. A dynamic binding mode with fluctuating hydrogen bonds between receptor and ligand offers a solution to cope with the high flexibility of the odorant ligand.[47]. Thus, we investigated the hydrogen bond contact frequencies between amylbutyrate and Ser263$^{6.51}$, Ser264$^{6.52}$, and Thr279$^{7.42}$, by classifying hydrogen bonds as robust (present in 100–50% of the simulated time), fluctuating (49–25%), and temporary (24–1%). We analyzed the A104G, A104I, F206V, V260W, S263C, S263V, S264C, S264V, and T279V mutants in 10 ns free MD simulations in the appropriate membrane/solvent environment (Supporting Information, Figure S4), comparing them

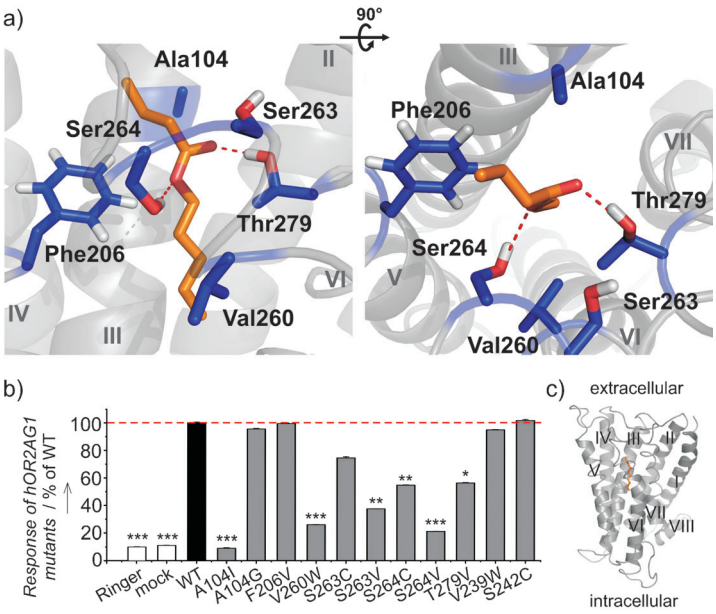

Figure 1. Characterization of the amylbutyrate-binding niche. a) Close-up of the putative ligand-binding niche of amylbutyrate bound to hOR2AG1 in the vertical binding mode after 10 ns free MD simulation. Ligand contact residues in blue, transmembrane helices (TMs) in gray. b) The effects of amino acid mutations in TM III, V, VI, and VII on receptor activation as measured by Ca^{2+} imaging of Hana3a cells expressing hOR2AG1 variants. The bar chart illustrates relative receptor activation by amylbutyrate (600 μM). Mean receptor activation (response probability) was normalized to response probabilities of wild type (WT) hOR2AG1-expressing cells (black bar). Error bars indicate the standard error of the mean (SEM). The data are representative of 15–40 independent experiments, each with 600–1600 cells. Significance according to Student's t-test relative to the amylbutyrate response probability of WT hOR2AG1 (*$P<0.05$, **$P<0.01$, ***$P<0.001$). Amylbutyrate application did not induce an increase in the cytosolic Ca^{2+} concentration in mock-transfected cells that was larger than the spontaneous activity induced solely by the application of Ringer's solution (white bars). c) Computer model of hOR2AG1 (gray) with amylbutyrate (orange sticks). The ligand is bound between helices III, V, VI, and VII in a binding mode vertical to the membrane plane.

Table 1: Computed hydrogen-bond contacts of amylbutyrate with hOR2AG1 variants. The frequency of hydrogen-bond contact occurrence is shown as percentage of the 10 ns simulated time.

hOR2AG1 variant	Hydrogen-bond contacts during MD simulation			Activity rating[a]	In vivo activity
	Ser263$^{6.51}$	Ser264$^{6.52}$	Thr279$^{7.42}$		
WT	12%	6%	92%	active	active
A104G	10%	8%	87%	active	active
A104I	66%	6%	43%	–	–
F206V	3%	40%	61%	active	active
V260W	11%	–	94%	–	–
S263C	2%[b]	2%	98%	active	active
S263V	–[b]	41%	74%	–	–
S264C	6%	–[b]	91%	–	–
S264V	4%	–[b]	19%	–	–
T279V	60%	35%	–[b]	–	–

[a] Temporary hydrogen bonding (>0%) to Ser263$^{6.51}$, Ser264$^{6.52}$ and robust hydrogen bonding (>49%) to Thr279$^{7.42}$ were considered as activity criterion. [b] Mutation affects respective amino acid residue.

with the mutant receptor activation by amylbutyrate. In simulations of all mutant receptors, which were still functional in experimental analysis (see Figure 1b), Ser263$^{6.51}$ and Ser264$^{6.52}$ established at least temporary hydrogen bonds with the ligand (during 2–66% of simulation time, see Table 1), and Thr279$^{7.42}$ showed a robust hydrogen bond (61–98% of simulated time, Table 1). The model also accounts for the remaining activity of the S263C mutant, as Cys263 still forms hydrogen bonds to amylbutyrate. We hypothesize that the dynamic hydrogen-bonding pattern of the ligand's ester group to these three polar residues, especially Thr279$^{7.42}$, serves as a criterion for receptor activation. A similar binding mode of a protein with an acetyl ester can be found in the crystal structure of the *Drosophila melanogaster* odorant binding protein LUSH (protein data bank (PDB) code: 2GTE; 1.4 Å; see Supporting Information, Figure S5 and Section 4).[48]

To further validate the proposed binding niche, we investigated if hydrogen bonds to Ser263$^{6.51}$, Ser264$^{6.52}$, and Thr279$^{7.42}$ can be used to predict the binding and activation properties of novel ligands. Therefore, we focused on five ester odorants (Figure 2a) that are structurally related to amylbutyrate. After superposition of the ligands of interest over amylbutyrate in the vertical binding mode (for details see Supporting Information, Section 5a), binding to the hydrophilic belt of hOR2AG1 (Ser263$^{6.51}$, Ser264$^{6.52}$, and Thr279$^{7.42}$) was assessed in 10 ns of free MD simulations (Supporting Information, Table S1). Comparison of simulations of the full ligand set in the WT protein with 10 ns and 100 ns trajectory length (Supporting Information, Table S1) showed that 10 ns of simulation is sufficient for sampling the contacts between protein and ligand in our model (for details see Supporting Information, Section 5b). We investigated whether the ligands can form temporary hydrogen bonds to Ser263$^{6.51}$ and Ser264$^{6.52}$ and robust hydrogen bonds to Thr279$^{7.42}$ during simulations in at least one of the employed orientations. While phenylethylacetate and phenirate fulfilled our activity criterion, prenylacetate, isoamylbenzoate, and isopentylacetate failed to do so (Figure 2a). The simulations were then compared to Ca^{2+} imaging measurements analyzing relative changes in hOR2AG1 activation potencies of tested odorants compared to amylbutyrate. In agreement with the simulations, phenylethylacetate and phenirate were experimentally found to be as active as amylbutyrate, whereas prenylacetate and isoamylbenzoate were significantly less active. Isopentylacetate had a reduced activity in comparison to amylbutyrate, though a t-test showed no significance for this result (Figure 2b). Other substances that were tested experimentally for hOR2AG1 activation are listed in the Supporting Information, Figure S6. Thus, MD simulations predicted the activity of five novel odorants qualitatively correctly. Earlier receptor-based approaches for the analysis of receptor/odorant pairs employed docking methods,[12–21] and could therefore only predict if a ligand sterically fits into a binding cavity. In our study, all six investigated odorants fit into the cavity, but only three out of six could fully activate the receptor. This was exactly predicted by our dynamic homology modeling approach, as it takes the dynamic interplay between ligand and receptor into account.

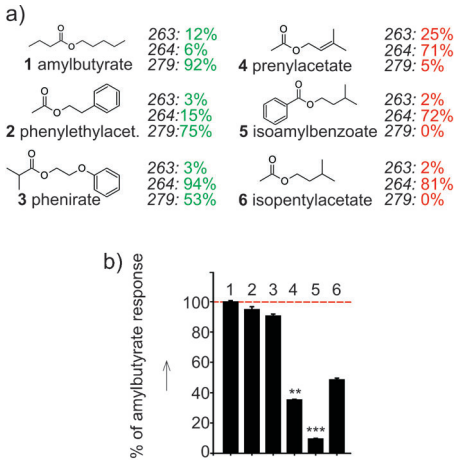

Figure 2. Ligand spectrum of hOR2AG1. a) Structurally related odorants were individually tested computationally for fulfillment of the activation criterion for hOR2AG1 using amylbutyrate as a template. The computed activity was judged by the capability to form hydrogen bonds with Ser263$^{6.51}$, Ser264$^{6.52}$, and Thr279$^{7.42}$ (italics) during MD simulations. Established hydrogen bonds are indicated as present at a percentage of simulation time. b) Bar chart illustrating relative hOR2AG1 activation potency by different odorants in Ca^{2+} imaging of Hana3a cells expressing recombinant hOR2AG1. The response probability to each odorant as a measure of receptor activation is indicated as the mean, normalized to the cellular responses to amylbutyrate. Non-specific cellular activation by respective odorants (as measured in mock-transfected cells) was subtracted. The data are representative of 12–40 independent experiments, each with 600–1600 cells. Bars indicate SEM. $^{**}P<0.01$, $^{***}P<0.001$ according to Student's t-test, all sample groups referred to cellular responses to amylbutyrate.

Analyzing our results, we propose a ligand selectivity filter for the recognition of a minimal distinct local molecular shape, a so-called odotope,[10] in hOR2AG1. The binding niche contains two hydrophobic cavities connected via a belt

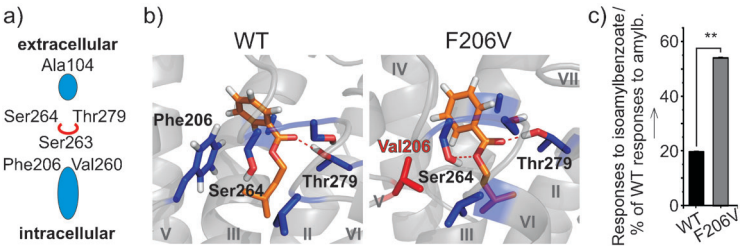

Figure 3. Reprogramming the hOR2AG1 selectivity filter. a) Scheme of the selectivity filter in hOR2AG1. Phe206$^{5.47}$ and Val260$^{6.48}$ form a size-selective filter close to the hydrophilic belt of Ser263$^{6.51}$, Ser264$^{6.52}$, and Thr279$^{7.42}$. b) Targeted computed altering of the proposed selectivity filter of hOR2AG1. TMs are shown in light gray, ligand contact residues in blue, Val206 in red. In contrast to the wild type (WT) protein, isoamylbenzoate forms hydrogen contacts to the hydrophilic belt, these contacts are predicted to be necessary for activation in the F206V mutant. c) Responses of recombinant hOR2AG1-F206V to isoamylbenzoate compared to that of WT hOR2AG1 as examined by Ca^{2+} imaging. The response probabilities to isoamylbenzoate were normalized to the WT response probability to amylbutyrate (amylb.). Bars indicate SEM, $^{**}P<0.01$ according to Student's t-test.

of hydrophilic residues (Ser263$^{6.51}$, Ser264$^{6.52}$, Thr279$^{7.42}$; Figure 1a and Figure 3a). Ala104$^{3.32}$ is in van der Waals contact with the cytoplasmic hydrophobic cavity, which is large enough to incorporate a methyl to propyl group. The hydrophilic belt itself is selective for the recognition of an ester moiety. Phe206$^{5.47}$ and Val260$^{6.48}$ form a size selective filter close to the hydrophilic belt, so that next to the ester moiety of the ligand, only unbranched methylene groups can exist. Larger residues, for example, a phenyl group, form repulsive van der Waals interactions with Phe206$^{5.47}$, which prevent the formation of hydrogen bonds with the hydrophilic belt. In the cytosolic cavity, large hydrophobic residues are tolerated (Supporting Information, Figure S7a), as is the case for phenylethylacetate. This filter may allow the receptor to be activated by multiple compounds, as long as they exhibit the R-CH_2-COO-CH_2-R′ odotope. There seems to be a maximal side-chain size, as compounds such as alusat, hexylacetate, and allylheptanoate, which all contain the odotope, cannot activate the receptor (compare Supporting Information, Figure S6). Phenirate is an exception, because its binding mode differs from amylbutyrate by forming hydrogen bonds with the hydrophilic belt through ester and ether moieties in parallel (Supporting Information, Figure S7b). Possibly, this ability to bind in a different binding mode may explain why for this ligand, an isopropyl group next to the ester moiety is tolerated.

Ligand-based methods showed a good performance to discriminate between activating and inactive ligands for other olfactory receptors, and could even elucidate the structure of new odorants.[8–10,22] To cross-check if the six ligands used in this study could reveal their activation potency by such an approach, we created pharmacophore models for the ligands with the help of the PharmaGist webserver.[49] The derived pharmacore model could identify all investigated ligands as putative binders for hOR2AG1, but could not distinguish between active and inactive compounds (see Supporting Information, Section 5c, Figure S12 and Table S3), either due to the small size of our employed ligand set, or because hOR2AG1 can distinguish between very small differences in the ligand scaffold. We therefore continue our investigation with our receptor-based "selectivity filter" model.

A very sensitive test for the selectivity filter is the introduction of a mutation, which can change the selectivity filter in a predictable way.[19] Isoamylbenzoate, which was found to be inactive in experimental analysis (Figure 2b), cannot bind the hydrophilic belt of WT hOR2AG1 owing to steric hindrance by Phe206$^{5.47}$. However, mutation to valine results in the required hydrogen bonding to all three hydrophilic residues in simulations of isoamylbenzoate in the F206V mutant (Figure 3b and Supporting Information, Table S1,). In agreement with this expectation, the F206V mutant showed a significant increase in receptor activation by isoamylbenzoate compared to the WT receptor (Figure 3c), whereas the amount of expressed protein remained unchanged (Supporting Information, Figure S8c). Thus, we can selectively alter receptor function based on computational information on the proposed binding niche by site-specific point mutation.

We extended our results with hOR2AG1 to predict ligands for orphan ORs. If the identified constellation of ligand-binding residues generally plays a role in ester recognition, ORs with the same amino acids in corresponding positions should also be able to be activated by amylbutyrate. We tested this hypothesis by modeling and functionally characterizing hOR2AG2 and mOR283-2, and could identify amylbutyrate as ligand for both ORs (Supporting Information, Figure S9 and Section 5d).

In conclusion, by combining dynamic homology modeling with site-directed mutagenesis and functional analysis, we provided a molecular model of the ligand-binding niche of hOR2AG1 within a receptor model. We could deduce a quantitative criterion for receptor activation by ligands based on computed hydrogen-bond contact frequencies to amino acids forming the ligand binding site. This information on the ligand selectivity filter in hOR2AG1 helped us to get insight into detection and discrimination of volatile, highly hydrophobic, and flexible ligands by olfactory receptors. Thereby, we were able to predict the activation capability of novel odorants. The dynamic model correctly predicts alterations in receptor function upon mutation for activation by ligands that do not activate the WT protein. Dynamic homology modeling may be applied in the future for deorphanization of ORs and to provide a valid basis for OR-based drug design.[42,43,50]

Received: June 10, 2011
Revised: October 10, 2011
Published online: December 5, 2011

Keywords: fragrances · functional characterization · molecular dynamics · molecular modeling · receptors

[1] S. Zozulya, F. Echeverri, T. Nguyen, *Genome Biol.* **2001**, *2*, research0018.1–00118.12.
[2] J. Bockaert, J. P. Pin, *EMBO J.* **1999**, *18*, 1723–1729.
[3] T. S. McClintock, T. M. Landers, A. A. Gimelbrant, L. Z. Fuller, B. A. Jackson, C. K. Jayawickreme, M. R. Lerner, *Mol. Brain Res.* **1997**, *48*, 270–278.
[4] K. Touhara, *Neurochem. Int.* **2007**, *51*, 132–139.
[5] B. Malnic, J. Hirono, T. Sato, L. Buck, *Cell* **1999**, *96*, 713–723.
[6] L. Buck, R. Axel, *Cell* **1991**, *65*, 175–187.
[7] G. Schneider, U. Fencher, *Nat. Rev. Drug Discovery* **2005**, *4*, 649–663.
[8] M. Schmuker, G. Schneider, *Proc. Natl. Acad. Sci. USA* **2007**, *104*, 20285–20289.
[9] M. Schmuker, M. de Bruyne, M. Hähnel, G. Schneider, *Chem. Cent. J.* **2007**, *1*, 11.
[10] G. Sanz, T. Thomas-Danguin, H. el Hamandi, C. Le Poupon, J. C. Pernollet, E. Guichard, A. Tromelin, *Chem. Senses* **2008**, *33*, 639–653.
[11] A. S. Nichols, S. Chen, C. W. Luetje, *Chem. Senses* **2011**, *36*, 781–790.
[12] M. S. Singer, *Chem. Senses* **2000**, *25*, 155–165.
[13] W. B. Floriano, N. Vaidehi, W. A. Goddard, M. S. Singer, G. M. Shepherd, *Proc. Natl. Acad. Sci. USA* **2000**, *97*, 10712–10716.
[14] N. Vaidehi, W. B. Floriano, R. Trabanino, S. E. Hall, P. Freddolino, E. J. Choi, G. Zamanakos, W. A. Goddard, *Proc. Natl. Acad. Sci. USA* **2002**, *99*, 12622–12627.
[15] W. B. Floriano, N. Vaidehi, W. A. Goddard, *Chem. Senses* **2004**, *29*, 269–290.

[16] S. E. Hall, W. B. Floriano, N. Vaidehi, W. A. Goddard, *Chem. Senses* **2004**, *29*, 595 – 616.
[17] T. Abaffy, A. Malhotra, C. W. Luetje, *J. Biol. Chem.* **2007**, *282*, 1216 – 1224.
[18] K. Khafizov, C. Anselmi, A. Menini, P. Carloni, *J. Mol. Model.* **2007**, *13*, 401 – 409.
[19] S. Katada, T. Hirokawa, Y. Oka, M. Suwa, K. Touhara, *J. Neurosci.* **2005**, *25*, 1806 – 1815.
[20] L. Doszczak, P. Kraft, H. P. Weber, R. Bertermann, A. Triller, H. Hatt, R. Tacke, *Angew. Chem.* **2007**, *119*, 3431 – 3436; *Angew. Chem. Int. Ed.* **2007**, *46*, 3367 – 3371.
[21] K. Schmiedeberg, E. Shirokova, H. P. Weber, B. Schilling, W. Meyerhof, D. Krautwurst, *J. Struct. Biol.* **2007**, *159*, 400 – 412.
[22] N. Triballeau, E. Van Name, G. Laslier, D. Cai, G. Paillard, P. W. Sorensen, R. Hoffmann, H. O. Bertrand, J. Ngai, F. C. Acher, *Neuron* **2008**, *60*, 767 – 774.
[23] K. Palczewski et al., *Science* **2000**, *289*, 739 – 745.
[24] T. Okada, M. Sugihara, A. N. Bondar, M. Elstner, P. Entel, V. Buss, *J. Mol. Biol.* **2004**, *342*, 571 – 583.
[25] V. Cherezov et al., *Science* **2007**, *318*, 1258 – 1265.
[26] S. G. Rasmussen et al., *Nature* **2007**, *450*, 383 – 387.
[27] M. Murakami, T. Kouyama, *Nature* **2008**, *453*, 363 – 367.
[28] V. P. Jaakola, M. T. Griffith, M. A. Hanson, V. Cherezov, E. Y. Chien, J. R. Lane, A. P. Ijzerman, R. C. Stevens, *Science* **2008**, *322*, 1211 – 1217.
[29] J. H. Park, P. Scheerer, K. P. Hofmann, H. W. Choe, O. P. Ernst, *Nature* **2008**, *454*, 183 – 187.
[30] T. Warne, M. J. Serrano-Vega, J. G. Baker, R. Moukhametzianov, P. C. Edwards, R. Henderson, A. G. Leslie, C. G. Tate, G. F. Schertler, *Nature* **2008**, *454*, 486 – 491.
[31] B. Wu et al., *Science* **2010**, *330*, 1066 – 1071.
[32] E. Y. Chien et al., *Science* **2010**, *330*, 1091 – 1095.
[33] O. Baud, S. Etter, M. Spreafico, L. Bordoli, T. Schwede, H. Vogel, H. Pick, *Biochemistry* **2011**, *50*, 843 – 853.
[34] V. Katritch, M. Rueda, P. C. Lam, M. Yeager, R. Abagyan, *Proteins Struct. Funct. Genet.* **2010**, *78*, 197 – 211.
[35] C. N. Cavasotto et al., *J. Med. Chem.* **2008**, *51*, 581 – 588.
[36] I. W. Davis, D. Baker, *J. Mol. Biol.* **2009**, *385*, 381 – 392.
[37] L. M. Simpson, I. D. Wall, F. E. Blaney, C. A. Reynolds, *Proteins Struct. Funct. Genet.* **2011**, *79*, 1441 – 14457.
[38] C. Hallmen, M. Wiese, *J. Comput.-Aided Mol. Des.* **2006**, *20*, 673 – 684.
[39] W. Fu, J. Shen, X. Luo, W. Zhu, J. Cheng, K. Yu, J. M. Briggs, G. Jin, K. Chen, H. Jiang, *Biophys. J.* **2007**, *93*, 1431 – 1441.
[40] S. Wolf, M. Bockmann, U. Howeler, J. Schlitter, K. Gerwert, *FEBS Lett.* **2008**, *582*, 3335 – 3342.
[41] E. M. Neuhaus, A. Mashukova, W. Y. Zhang, J. Barbour, H. Hatt, *Chem. Senses* **2006**, *31*, 445 – 452.
[42] M. Spehr, G. Gisselmann, A. Poplawski, J. A. Riffell, C. H. Wetzel, R. K. Zimmer, H. Hatt, *Science* **2003**, *299*, 2054 – 2058.
[43] E. M. Neuhaus, W. Zhang, L. Gelis, Y. Deng, J. Noldus, H. Hatt, *J. Biol. Chem.* **2009**, *284*, 16218 – 16225.
[44] J. A. Ballesteros, H. Weinstein, *Methods Neurosci.* **1995**, *25*, 366 – 428.
[45] O. Man, Y. Gilad, D. Lancet, *Protein Sci.* **2004**, *13*, 240 – 254.
[46] Y. Pilpel, D. Lancet, *Protein Sci.* **1999**, *8*, 969 – 977.
[47] Z. Peterlin, Y. Li, G. Sun, R. Shah, S. Firestein, K. Ryan, *Chem. Biol.* **2008**, *15*, 1317 – 1327.
[48] J. D. Laughlin, T. S. Ha, D. N. Jones, D. P. Smith, *Cell* **2008**, *133*, 1255 – 1265.
[49] D. Schneidman-Duhovny, O. Drod, Y. Inbar, R. Nussinov, H. J. Wolfson, *Nucleic Acids Res.* **2008**, *36(Web-Server issue)*, W223 – 228.
[50] M. Spehr, H. Hatt, *Drug News Perspect.* **2004**, *17*, 165 – 171.

